Research Article

Mario Mueh*, Robert Knieß*, H. Ulrich Göringer, and Christian Damm

Concepts for Millimeter Wave-based Detection of African Trypanosomes in Field-compatible Liquid Systems

https://doi.org/10.1515/sample-YYYY-XXXX
Received Month DD, YYYY; revised Month DD, YYYY; accepted Month DD, YYYY

Abstract:
Human African Trypanosomiasis (HAT) is caused by the African trypanosome, a single-cell parasite that proliferates in the blood and cerebrospinal fluid of infected patients. Diagnostic measures for this pathogen are currently not sufficiently robust and reliable enough to permit effective disease control procedures. As a consequence, we suggested the development of a new sensor type, combining the selectivity of parasite-specific nucleic acid aptamers with the sensitivity of resonant electromagnetic devices to capture and detect the disease-causing organism. While we accomplished the detection of parasite cells in dehydrated specimens, here we summarize our recent progress toward electromagnetic sensors capable of uncovering parasites in liquid patient samples. We present a technique for the removal of blood cells from blood specimens and the deposition of trypanosome cells on glass microfiber membranes for dielectric spectrometry. Liquid suspensions of trypanosomes are characterized to determine the actual dielectric properties of single parasites and lastly, we present two sensor concepts optimized for the detection in liquids, along with a fabrication technique for the integration of microfluidic sample confinements.

Keywords: Microwave sensors, terahertz, African Trypanosomes, biosensors, microfluidics, neglected diseases

1 Introduction

The lack of affordable and at the same time robust diagnostic tools in developing countries is a major hindrance for disease control [1]. This holds especially true for African trypanosomiasis, a parasitic disease, which is also known as African sleeping sickness [2]. Sleeping sickness has caused multiple epidemics during the 20th century and only in the last decade has the number of reported cases decreased [3]. Nonetheless, it is still present in parts of sub-Saharan Africa and there it remains an unremitting threat to more than 50 million people in more than 30 countries [3]. Also, the disease in domestic animals is highly damaging to the agricultural development of the continent. Importantly, sleeping sickness is fatal if left untreated [1, 2]. No vaccination exists and all available drugs are at best suboptimal [1, 3, 4]. This problem is further amplified by the fact that simple, accurate, and reliable diagnostic tests are by and large missing.

Trypanosomes are transmitted by tsetse flies. The parasites multiply in the peripheral blood and tissue fluids of an infected host, which represents the so-called haemolymphatic phase of the disease. It is characterized by fever attacks, headaches, and joint pains. After that, the parasites cross the blood-brain barrier to infect the central nervous system (CNS). This induces grave neurological symptoms such as sensory disturbances, confusion as well as a disturbance of the sleep cycle, hence the name sleeping sickness. Clinically, two forms of sleeping sickness are distinguished: A chronic form, which occurs in Central and West Africa that is caused by the parasite species *Trypanosoma brucei gambiense*. Second, an acute, inflammatory-type illness in East and Southern Africa induced by *Trypanosoma brucei rhodesiense*. The species *Trypanosoma brucei brucei* afflicts domestic and wild animals [5]. Diagnosis of the chronic form of the disease relies on laboratory examinations because clinical characteristics are often ambiguous. This includes simple microscopic inspections of lymph node aspirates, cerebrospinal fluid (CSF), and blood samples as well as various serological tests such as a card agglutination test (CATT), immunofluorescence and enzyme-linked immunosorbent assays (ELISA). Unfortunately, no serological tests for *T. b. rhodesiense* exist. The identification of the acute form relies on non-specific clinical symptoms only. Fortunately,

***Corresponding author: Mario Mueh, Christian Damm,** Ulm University, Institute of Microwave Engineering, Ulm, Germany, e-mail: {mario.mueh, christian.damm}@uni-ulm.de
***Corresponding author: Robert Knieß, H. Ulrich Göringer,** Technical University of Darmstadt, Molecular Genetics, Darmstadt, Germany, e-mail: {kniess, goringer}@bio.tu-darmstadt.de

the parasitological analysis is easier because the number of blood circulating parasites is higher. Nevertheless, all tests rely on the individual interpretation of laboratory and medical personnel and on visual comparisons with standard charts, thereby introducing a high level of uncertainty. As a consequence, the search for improved and technically robust diagnostic tests for the early detection of trypanosome infections has not subsided.

Following up on our previous work with sensor designs using dehydrated trypanosome cell material [6] here we describe our latest results from experiments aiming at the detection of trypanosomes in liquid samples to provide the ground for fieldwork measurements in biological fluids such as blood, lymph node aspirates and cerebrospinal fluid. For the electromagnetic detection of the parasite cell material, passive resonant metallic structures are used, which store and localize the energy of an incident electromagnetic wave in the minuscule sample volume formed by a low number of parasites in a bulk sample. A change in the local dielectric permittivity, caused by the interior composition of the cells, is translated to a change in the resonance spectrum of the sensor structure. This change is then externally detected. In addition, the properties of the participating media are a topic of interest as they form the dielectric environment and material contrast required for the detection. At the same time, the sensor device must be constructed such that the lossy aqueous medium does not extinguish its electromagnetic resonance.

2 Detecting African trypanosomes in Liquid Samples

2.1 Experimental setup and safety considerations

During the exploratory phase in the development of a sensor device for African trypanosomiasis, it is neither ethical nor prudent to rely on patient material to test and optimize the design layout. As a consequence, other means to generate the required parasite quantities must be found. Since African trypanosomes are hemoflagelates they are typically grown in the blood of inbred rat or mice strains that are maintained at defined laboratory conditions. Animals are typically intraperitoneally infected and the parasitemia is monitored by tail blood examinations. In such settings, parasites can reach cell densities of 1-5 $\times 10^8$ cells/mL. By contrast, infected humans who are diagnosed with sleeping sickness rarely show *T. b. rhodesiense* parasitemias above 10^6 parasites/mL, although some cases of 10^8 cells/mL

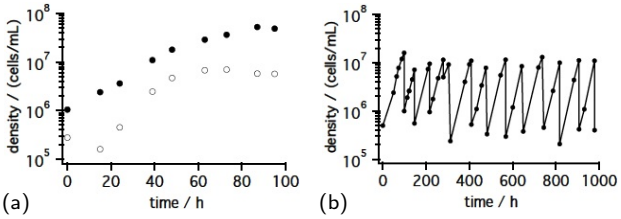

Fig. 1: (a) Growth curves of procyclic-stage (filled circles) and bloodstream-stage (open circles) *T. b. brucei* parasites. (b) Repetitive dilution of procyclic stage *T. b. brucei* parasites to maintain logarithmic growth.

have been reported. Since both, *T. b. rhodesiense* and *T. b. gambiense* are human pathogens, all laboratory procedures must be conducted at high safety levels to assure that the involved laboratory personnel is not at risk of contracting the disease.

In order to circumvent these hazards, we decided to use a laboratory strain of *Trypanosoma brucei brucei* for our experiments. *T. b. brucei* is the causative agent of the Nagana pest in southern and central Africa. Nagana represents the animal form of sleeping sickness and mainly affects cattle and horses but not humans. As such *T. b. brucei* can be considered a laboratory safety strain for the intended measurements. Furthermore, we used a monomorphic strain of *T. b. brucei*. Monomorphic parasites are not transmittable by insect vectors and as a consequence can be handled at low safety restrictions. In addition, the parasites can be inactivated by chemical fixation without altering their cellular composition. This provides a way of handling large volumes of parasite cells without any safety concerns. Both insect-stage, so-called procyclic trypanosomes, as well as mammalian bloodstream-stage trypanosomes were cultured in synthetic liquid media at axenic conditions. Under these conditions, the media composition mimics the nutritional needs of the parasites, although supplementation with 10 % (v/v) fetal bovine blood serum (FBS) is required to provide growth factors and lipids. Procyclic stage trypanosomes, which mainly use oxidative phosphorylation for energy production, were additionally supplemented with hemin. Figure 1a shows representative growth curves of both, procyclic and bloodstream-stage trypanosomes verifying the typical lag-, log- and stationary phases of healthy, proliferating cells. In the logarithmic phase, the doubling time for procyclic trypanosomes is $\leq$12 h (at 27 °C) and for bloodstream stage trypanosomes at 37 °C it is roughly 6 h.

We also tested that both parasite life cycle stages can repeatedly be diluted to keep the parasites in logarithmic

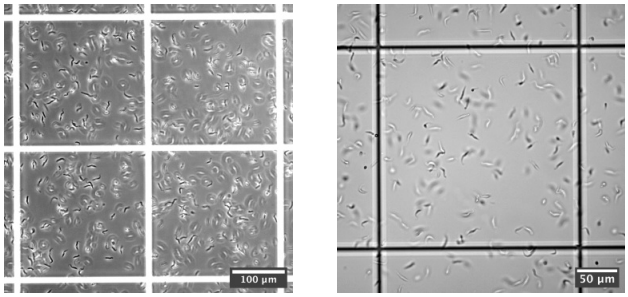

Fig. 2: Procyclic-stage *T. b. brucei* parasites at a cell density of 1.3×10^7 cells/mL in a Neubauer counting chamber. (a) phase-contrast microscopy. (b) brightfield microscopy.

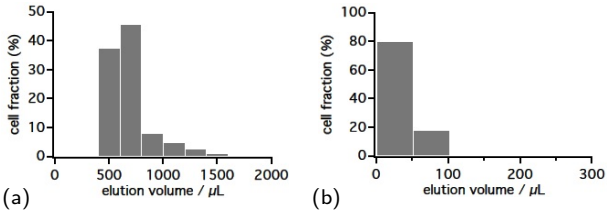

Fig. 3: (a) Isocratic gravity flow DEAE-anion-exchange chromatography of bloodstream-stage trypanosomes. Column bed volume 1.6 mL. Parasite cell number: 1×10^4 cells in 0.2 mL. (b) Spin-column format of the DEAE-anion exchange chromatography. DEAE bed-volume: 0.5 mL. Parasite cell number: 1×10^5 cells in 0.05 mL.

growth (Fig. 1b). As expected, *T. b. brucei* proliferating under such conditions shows the archetypical slender morphology of African trypanosomes, which is characterized by a cell width of 2 µm to 5 µm and a body length of 25 µm to 30 µm. Parasites were visualized by phase-contrast or brightfield light microscopy and cell numbers were counted either in standardized cell counting chambers (Fig. 2) or by automated cell counting. Typically, cell densities of $\geq 5 \times 10^7$/mL (procyclic) and $\geq 5 \times 10^6$/mL (bloodstream) were achieved.

A recent comparison of the transcriptomes of *Trypanosoma brucei rhodesiense* from blood and cerebrospinal fluid of human patients with those of trypanosomes from culture and rodents confirmed the overall metabolic identity of the parasites in the different environments [7] providing further justification for the above-described approach.

2.2 Removal of blood cells

A field-compatible analysis of trypanosome infections will have to be conducted from blood, lymph node aspirates, or cerebrospinal fluid specimens. Although blood samples are readily available even in rural, low-tech environments, they have the disadvantage of containing very high numbers of blood cells (5×10^9 cells/mL), mainly erythrocytes (>90 %), as a background. This is especially unfavorable at the early stages of an infection when parasite titers can be six orders of magnitude below the blood cell count. As a consequence, the removal of blood cells is indispensable for any "field-compatible" diagnostic approach. To experimentally address this issue, we relied on the highly validated anion exchange chromatography method first published by Sheila Lanham [8, 9]. The technique uses matrix-attached diethyl aminoethyl (DEAE)-groups as a capturing ligand, which at pH values between 6 to 9 binds all blood cell material by ionic interaction. Trypanosomes elute in the void volume with the blood plasma from which the parasites can be captured and further concentrated if necessary. We established that the Lanham setup can be used as an isocratic gravity-flow technique as well as in a spin-column format using low-speed ($1000 \times g$) centrifugation [8, 10] (Fig. 3). Both procedures yield highly enriched, erythrocyte-free parasite preparations, which can directly be fed into the electromagnetic detection workflow. Furthermore, both methods are highly reproducible, robust, and field-compatible, requiring only a minimal set of laboratory equipment [9].

2.3 Parasite deposition on glass-microfiber membranes

As an alternative to measuring parasite cells in a fully immersed liquid environment, we analyzed whether trypanosomes can be deposited onto solid materials with favorable permittivity characteristics to enable measurements in a hydrated but not fully immersed state. For that, we chose commercially available 0.2 mm-thick SiO_2 (glass) microfiber membranes with a defined pore size of 1.2 µm. Parasites were deposited at low hydrostatic pressure and since the microfiber pore size represents roughly 1/20-th the length of a parasite cell ≥95% retention of the applied cell matter was achieved. Figure 4 shows a representative example of the experimental setup using pre-stained trypanosomes as a model. Notably, the procedure is nondestructive for parasite cells. It is low-tech and as a consequence compatible with rural work conditions and it enables the generation of layers of cell material with adjustable surface densities ranging from only 2×10^2 parasites/mm^2 to $\geq 1 \times 10^6$ parasites/mm^2. Similarly, the hydration state of the samples can be varied between 0 %

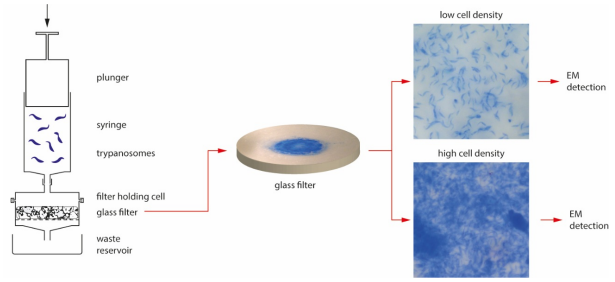

Fig. 4: Deposition of *T. b. brucei* parasites onto 0.2 mm thick glass-microfiber membranes using a syringe/filter-holder device. The pore size of the glass microfiber filters is 1.2 µm. Parasite cells are pre-stained with Brilliant blue G250 for visualization purposes only. Filters of low to high cell density per surface area can be generated.

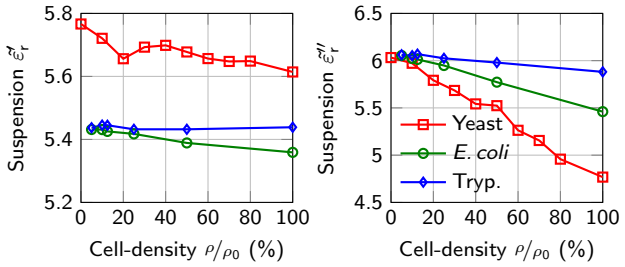

Fig. 5: Bulk permittivity of a sample containing yeast, *E. coli*, and trypanosome cells in varying cell-density ρ/ρ_0, each measured at 275 GHz. ρ_0 represents the different cell densities of the raw specimens. The increased real part of the yeast series originates from differences in the ambient temperature.

water content to 100 % humidity. Control glass microfiber membranes were generated with *E. coli* bacteria and yeast (*Saccharomyces cerevisiae*) cells.

3 Electromagnetic Sensing

3.1 The dielectric properties of trypanosome cell suspensions

As stated above, the detection of human pathogenic parasites in the body fluids of infected patients imposes a substantial number of safety constraints on the measurement setup. However, by using cultured parasite cells of the cattle pathogen instead of the human pathogen most safety considerations were sidestepped thereby allowing the handling of large numbers of parasite cells. Furthermore, measurements of single parasite cells were not considered feasible, because individual cells would have to be precisely confined to maximize the intersection of electromagnetic energy localization and cell volume. Therefore, bulk measurements are performed using cell suspensions of known cell densities. To match the salt concentration and osmolarity of the body fluids, phosphate-buffered saline (PBS) is used as the surrounding buffer solution. PBS does not exhibit any notable dielectric difference from pure H_2O and using the assumption that individual cells have distinct and anomalous dielectric properties, the electromagnetic characteristics of individual cells can be extracted by rarefaction of the cell suspension. All differences in cellular geometry and orientation are then averaged over the entire cell population. An RF-transparent precision chamber is used to enclose each parasite sample and initially, commercially available precision cavities designed for microscopy-based cell counting purposes (C-Chip) were used. Although the inner cavity dimensions were found to be highly accurate, the outer geometry, the material, and the casing/sample contrast ratio proved to be insufficient for reliable measurements. Instead, a custom-made glass cuvette is employed. Any temperature changes during the measurement are monitored by intermittently measuring a PBS-filled reference chamber in the same cuvette.

Measurements of suspended cells show a density-dependent reduction in the complex permittivity within the spectral range of 220 GHz to 330 GHz. For clarity reasons, only the 275 GHz results are shown (Fig. 5). Interestingly, the dielectric change mainly impacts the imaginary part of the complex permittivity, *i.e.* the RF-loss, whereas the real part remains almost constant. A similar result is obtained for suspensions of *E. coli* bacteria and baker's yeast (*Saccharomyces cerevisiae*). Unlike the trypanosome and *E. coli* specimen, the yeast cells are not fixated and thus are metabolically active, which clearly demonstrates that dielectric properties can be extracted from live-cell preparations. The full data set supports the observed permittivity constellation and dilution trend. However, the actual inner permittivity contributed by each species appears to differ slightly, most likely as a result of differences in water content and insoluble components. To derive the properties of single cells from bulk permittivity measurements, the density of the suspensions and the approximated average volume of a single cell is used to calculate an effective medium approximation. Given that the cell sizes (approx. length of *E. coli*: 2 µm; *T. brucei*: 30 µm) are far smaller than one wavelength in medium (ca. 430 µm at 300 GHz, $\varepsilon'_r \sim 5.5$ of H_2O) and assuming that the cells are evenly distributed, the Maxwell-Garnett approximation can be applied [11]. Although this approximation is only fully valid for low volume ratios of inclusion material to the surrounding host material, to avoid bunch-

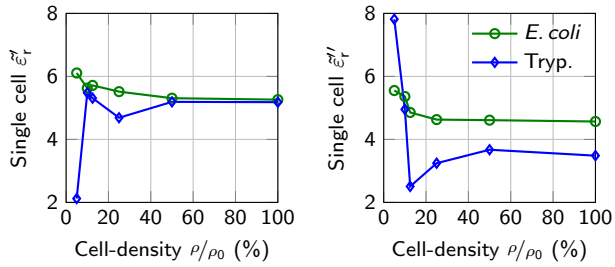

Fig. 6: Permittivity of single *E. coli* and trypanosome cells at 275 GHz, estimated from a reverse Maxwell-Garnett model. In the ideal case the values are independent of cell-density ρ/ρ_0. Towards zero density, measurement errors are amplified by projection onto a diminishing cell volume.

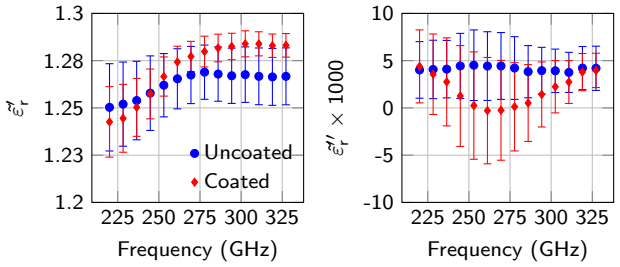

Fig. 7: Coated and uncoated glass microfiber filters: mean (marks) and standard deviation (error bars) of the real and imaginary relative permittivity over six samples per type.

related effects of closely-spaced particles, the difference in the real relative permittivity of particles and host is suspected to be small (<10 %), and the interaction potential among particles is therefore low. The results, shown in Fig. 6, indicate a significant difference of the imaginary part (*E. coli*: ∼25 %, trypanosomes: ∼40 %) in comparison to the buffer. This finding has important implications for sensor design, as it defines the expected dielectric contrast achievable by accumulating a volume of parasite cells. Knowing the inner permittivity, the properties of this aggregate is easily embedded in a full-wave simulation to predict the sensor response.

It also allows to estimate the expected sensitivity of a transmission-based sensing device and sets the frame for the required parasite cell densities. With the current characterization setup and no further stabilization measures, the detection limit is in the range of 7.7×10^7 parasites/mL or 10 % of ρ_0.

3.2 Characterization of trypanosome-coated glass microfiber membranes

Bio-materials deposited on thin carrier films can be characterized, as shown in our publication on the dielectric properties of dried films of parasite cells [12]. The nature of the carrier plays an important role in the reliability and stability of the resulting data. To extract the properties of the deposited material, it is necessary that the thickness and effective electromagnetic properties of the carrier are known. This is easily accomplished for solid glass wafers and polymer films. However, the properties of glass microfiber membranes are not fixed since the material is porous and compressible (ca. 30 %). To evaluate if trypanosomes deposited on glass microfiber membranes can be detected by continuous-wave RF transmission, cell layers with surface densities of 2×10^5 parasite cells/mm^2 are analyzed. Empty filter membranes are used to determine the properties of the bare glass matrix. Measurements are performed in a non-hydrated state with six individual membranes for each condition. The resulting permittivity data show no clear difference between the cell-coated and bare filter membranes (Fig. 7). However, the data points do show a systematic deviation. As this experiment is performed in a continuous-wave (CW) transmission instrument at 220 GHz to 330 GHz, the target signal may be masked by path reflections of the setup. A more detailed analysis using time-domain spectrometry is expected to clarify this issue. However, the data indicate that dried-state trypanosomes do not provide sufficient dielectric change for a reliable detection within this setup. To consider the filter-matrix as a platform for parasite detection, it is therefore crucial to determine whether gradually rehydrated trypanosomes regain the dielectric properties of fully hydrated cells to increase the signal to a detectable range.

3.3 Design concepts

Aside from the difficulty imposed by the dielectric similarities of cell and medium, another problem arises in the form of a strong RF loss. Passive RF structures for the examination of small volume quantities – like resonator circuits – usually rely on remote excitation to eliminate the need for contacts and to allow for a higher concentration of the electromagnetically stored energy. However, the detection of changes within this measurement system requires that the spectral imprint of a resonance – resulting from wave interference, coupling strength and loss – is detectable in the return signal by sufficient depth and sharpness of the feature. When an aqueous medium is in proximity to the sensor, the resonance feature broadens

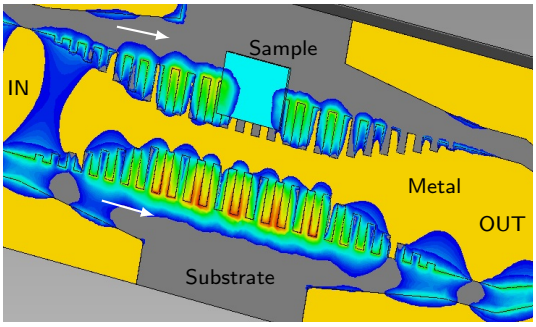

Fig. 8: Differential planar plasmonic edge waveguide, equally splitting a coplanar waveguide into two individual plasmonic launches. Each wave propagates through the measurement zone before recombining into a CPW mode. Changes of the propagation constant by dielectric material in one branch (light-blue block) strongly influence the resulting output mode.

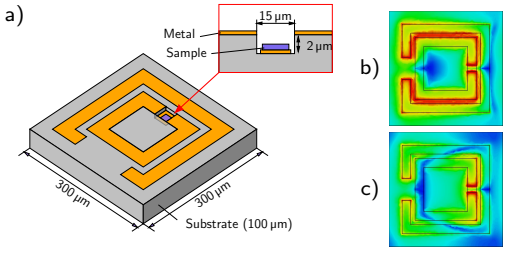

Fig. 9: a) Multi-resonant sensor element designed for location-dependent sensitivity inside or outside of the detection zone (shown in the inset)[13]. The electric field distribution in b) the area-sensitive 1st mode and c) the target-localized 2nd resonance mode determines the response to target or spurious material.

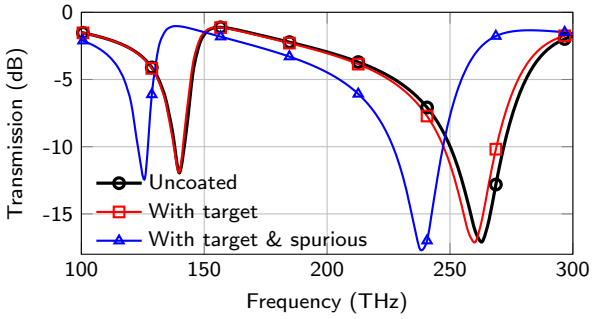

Fig. 10: Exemplary transmission spectrum of the multi-resonant sensor, showing the 1st (140 GHz) and 2nd (260 GHz) resonance mode in different loading scenarios. If loaded with target material in the detection zone, only the 2nd mode responds. Spurious deposits covering the remaining surface impact both modes.

and loses depth: the stronger the electric field is confined into the lossy medium, the higher the attenuation.

Generally, the amount of aqueous medium interacting with the sensor element must be limited to the required minimum. A full-surface application of the sample is therefore not feasible; its extent must be restricted.

For dry and partially hydrated materials, resonant sensors have proven to be highly sensitive to changes in very small (∼3.5 pL per resonator) dielectric volumes. However, approaches targeted to detect changes in the real part of the permittivity miss out on the actual change in the imaginary part, as indicated by our measurements. In aqueous media, the evaluation of the signal by resonance strength/quality is therefore superior to the detection of a resonance shift evoked by a change in the real permittivity. Two concepts for different designs were investigated to this end. The first design is a differential plasmonic waveguide (Fig. 8) highly sensitive to materials in proximity to the resonant waveguide structure. This design requires galvanic contact and has so far been evaluated in simulation only. The second design uses a split-ring resonator with either embedded microfluidic channels (Fig. 11a) or a structured coating layer, which allows liquids to remain only in precisely defined regions (Fig. 11b). These regions can be functionalized with haptophoric molecules such as nucleic acid (DNA or RNA) aptamers or antibodies as suggested in [6]. This design is intended for free-space coupling and has been investigated on the basis of a prototype.

In addition to the selectivity introduced by a haptophoric surface, the sensor device should display an inherent selectivity to common sources of measurement error. A problematic aspect is the homogeneity of the "loading", *i.e.* the deposited material-under-test. By the nature of non-equilibrium and multi-modal binding characteristics of biological material (*e.g.* hydrophobic, ionic, and dipolar interactions), specific and unspecific binding to the sensor will occur. Therefore, inhomogeneous occupation of the detection fields is expected. Since the sensor is usually designed for a specific loading strategy, the resulting measured value would lose its significance.

A possible solution encompasses the use of not one but multiple resonances of a single resonator design. Since each resonance mode produces a different field distribution above a single resonator element, the sensitivity in the respective mode depends on the location of the deposited material. We presented such a design (Fig. 9a) [13], which utilizes two modes to address either the actual binding site for parasites (Fig. 9c) or the surrounding area (Fig. 9b). By comparing the shift of both resonance frequencies observed in the transmission spectrum (Fig. 10), the deposition pattern can be qualified. Thus, measurements indicating off-site binding of parasites can be detected and eliminated automatically. This concept was demonstrated and optimized in full-wave simulations of a single resonator in [13]. The results of this simulation study

Tab. 1: Multiresonant split-ring sensor tuned for loading qualification: Experimentally determined sensitivity and standard deviation on a $20 \times 20\text{mm}^2$ sensor, compared to desired margins determined by full-wave simulation. Three modes are included, as the sensor can be evaluated using either 1st and 2nd, or 2nd and 3rd mode.

Mode #	Target sensitivity (%)		Spurious sensitivity (%)	
	Goal	Measured	Goal	Measured
I	0	0.1 ± 0.1	≤ -10	-14.5 ± 1.2
II	≤ -0.5	-0.5 ± 0.2	≤ -10	-13.3 ± 2.0
III	0	0.1 ± 0.1	≤ -10	-9.4 ± 2.8

were then evaluated for the lowest expected permittivities of a localized cell-film equivalent (photoresist, $\varepsilon'_r \sim 2.5$) and of a common spurious residue (low-density buffer salt crystals, $\varepsilon'_r \sim 2.5...4$) to obtain a set of minimum validation goals, listed in Tab. 1. A follow-up experiment, included in Tab. 1, has since confirmed these predicted sensitivities to each scenario almost perfectly. In the measurement, a $20 \times 20\text{mm}^2$-large array of identical resonators was evaluated element-wise, yielding a set of individual measurements for a statistical evaluation. Measurements included the uncoated array, the added local photoresist coating, and the added salt crystal overcoat.

3.4 Fabrication of sensor devices

Dielectric sensing devices implemented in microfluidic systems have been used in the past, usually with the drawback of a second material layer of different composition, which is bonded to the RF device. Microfluidic systems can be implemented into the sensing device with *e.g.* imprinted polymers, 3D-printed or laser-engraved materials, or photo-structured films [14]. However, the integration of height variations in the RF substrate adds additional degrees of freedom to the design by placing electrodes at different height levels [15, 16]. In addition, the integration of channeling structures for liquid media directly into the RF substrate potentially eliminates the need for a second, structured layer and allows for a more homogeneous material composition.

Since we have found polyethylene terephthalate (PET) films to be a suitable substrate for thin and durable passive circuits at THz frequencies, an additional processing step has been added to enable selective etching of the polymer surface [17]. For this purpose, a modified microstructuring workflow was devised, which first defines the RF metallization, before another metallization layer is added on top to serve as an etch resist mask. By applying oxygen reactive-ion etching (O_2-RIE) the exposed PET

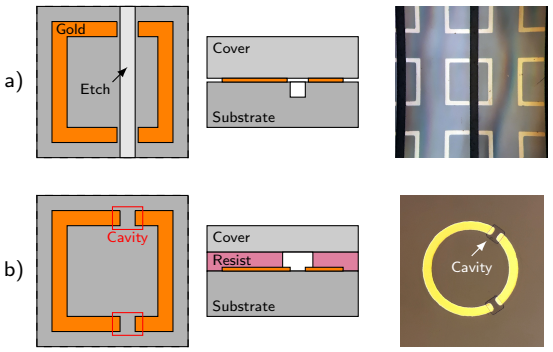

Fig. 11: Concepts for fluid confinement on sensor device: Etched microchannel (a) and structured resist microcavity layer (b), shown as schematic in top-down (left) and cross-section views (middle), and actual device micrographs (right).

surfaces are then eroded, leaving an imprint of the mask to the desired depth. While the edges of this imprint are superbly defined (deviation usually smaller than 0.5 µm) due to the anisotropic (*i.e.* surface-perpendicular) etching reaction, the floor of the etched areas remains rough as a result of nano-thread formation caused by surface chemistry changes during the oxygen-ion bombardment [18]. Such surfaces have been found to exhibit a significantly improved wettability compared to bare PET, thus aiding the distribution of liquid. This technique was demonstrated on prototype sensors in [17], consisting of split-ring resonator arrays with channels crossing the resonator gaps as shown in Fig. 11a, including inlet and outlet distribution networks to establish an even pressure distribution over all channels. RF measurements of the prototype showed a distinguishable resonance profile [17], although the overall loss was higher than anticipated from full-wave simulations; this is most likely a technical problem requiring fine-tuning of the oxygen etching procedure. To further reduce RF losses an improved concept is being investigated, including a protective polymer coat over the split-ring matrix with the exception of the detection zones (Fig. 11b). This layer is intended to displace superfluous liquid from the immediate vicinity of each resonator.

In summary, the sensor package will have a strong influence on the output signal reliability. Ideally, the sensitive element is enclosed as illustrated in Fig. 12, with liquid insertion ports being integrated to load the sensor by self-distribution, *e.g.* by capillary force. Practical applications could encompass the subsequent propagation of activation agents, sample fluid, and rinse liquids through the cavity in a well-defined manner. Both of the aforementioned sensor concepts are suitable for this approach, albeit a contact-free design is preferred for its lower complexity and thus better read-out reliability.

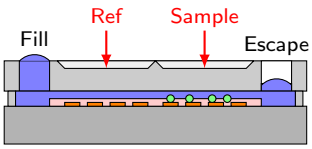

Fig. 12: Promising packaging concept: Fused polymer films enclosing a sensor matrix with cavity cladding, isolating the sensor from environmental factors and enabling capillary distribution of the sample. Red arrows mark the RF probe windows.

4 Conclusion

We have summarized our progress towards aptamer-based sensors for the detection of African trypanosomes in aqueous samples. As a first approach, we have demonstrated a technique for the isolation and deposition of trypanosomes on glass microfiber membranes. However, dielectric spectrometry indicates yet an insufficient material contrast of the dehydrated parasites for a reliable detection. For the second approach, we have presented measurements of dielectric properties of single trypanosomes, *E. coli* bacteria, and baker's yeast cells, derived from characterizations of bulk suspensions. From the resulting data sets we have derived two improved concepts for electromagnetic sensors capable of operating in contact with liquid media. First, a differential plasmonic waveguide, providing high sensitivity to surface-deposited media and simple read-out where the interaction mechanism must still be refined. Second, the integration of microfluidic system components with an optimized resonator matrix sensor, reducing the liquid volume overhead and thus the RF loss.

In the future, we will combine the deposition on glass microfiber membranes with the superior sensitivity of time-domain spectrometry. The individual sensitivity of the two demonstrated electromagnetic sensor types will be fine-tuned. Their performance will be tested with parasites deposited by binding to aptamer-functionalized sites. At this point, a comparison to state-of-the-art HAT diagnostics appears feasible. Finally, a packaged sensor device will be developed.

Material and Methods

Cell material

Procyclic-stage *Trypanosoma brucei brucei*, strain Lister 427 [19]. Bloodstream-stage *Trypanosoma brucei brucei* strain Lister 427, MITat serodeme, variant clone MITat 1.2 [19]. *Escherichia coli* strain DH5α (F^- endA1 glnV44 thi-1 recA1 relA1 gyrA96 deoR nupG purB20 φ80 ΔlacZ ΔM15 Δ(lacZYA-argF)U169, hsdR17(rK^-mK^+), λ^-) [20]. *Saccharomyces cerevisiae* strain W303-1A (MATa leu2-3,112 trp1-1 can1-100 ura3-1 ade2-1 his3-11,15) [21].

Cell culture methods

Procyclic-stage trypanosomes were cultured in SDM79-medium [22] supplemented with 10 % (v/v) fetal bovine serum, 50IU/mL penicillin, 50 µg/mL streptomycin, and 7.5 µg/mL hemin at 27 °C. Bloodstream-stage trypanosomes were cultured in HMI9-medium [23] supplemented with 10% (v/v) fetal bovine serum, 0.2mM 2-mercaptoethanol, 100 IU/mL penicillin, 100 µg/mL streptomycin at 37°C in 5 % CO_2 and ≥95 % relative humidity. *E. coli* bacteria were grown in LB-broth containing 10 g/L tryptone, 5 g/L yeast extract, and 5 g/L NaCl at 37 °C with constant shaking. Yeast cells were cultured in YPD-medium (10g/L yeast extract, 20g/L peptone, and 20g/L glucose) at 25°C with constant shaking. Cells were grown to the diauxic phase ($\sim 1\times10^8$ cells/mL) and harvested by centrifugation. Cells were washed (2x) with 20 vol. dH_2O and resuspended to a cell density of $\sim 1 \times 10^9$ cells/mL.

Cell preparation for liquid measurements

Procyclic-stage trypanosomes at 1.5×10^7 cells/mL and *E. coli* bacteria at 4×10^9 cells/mL were harvested by centrifugation and suspended in PBS buffer pH7.4 (10mM Na_2HPO_4, 1.8mM KH_2PO_4, 137mM NaCl, 2.7mM KCl). Cells were treated with 15 vol. ice-cold 99% (v/v) MeOH and were resuspended in PBS buffer to final cell densities of 2.4×10^{11} cells/mL for *E. coli* and 7.7×10^8 cells/mL for trypanosomes.

Anion-exchange chromatography

Diethylaminoethyl (DEAE) trisacryl Plus M anion-exchange material (Sigma), with a bead size of 40 µm to 80 µm, was equilibrated in phosphate buffer (67mM $Na_xH_yPO_4$ pH8.1, 44mM NaCl, 1 % (w/v) glucose). Columns were packed for either gravity-flow (Polyprep, Bio-Rad) with 1.6 mL bed volume or for centrifugation (Micro Bio-Spin, Bio-Rad) with 0.5 mL bed volume of DEAE-material. Bloodstream-stage trypanosomes were taken from stationary cultures ($2–4\times10^6$/mL) and diluted in HMI9-medium. For gravity-flow experiments, 1×10^4 cells in 0.2 mL were applied to the DEAE-material. Phos-

phate buffer was continuously added and 0.2 mL fractions were collected. Cells in the fractions were pelleted by centrifugation and suspended in <0.02 mL of supernatant. Cell counting in a Neubauer chamber determined the number of cells in each fraction. For the spin-column setup, 1×10^5 cells in 0.05 mL were applied to the DEAE-material. Columns were centrifuged at $1000 \times g$ for 1 min at 4 °C, and the flow-through was collected. Columns were repetitively loaded with 0.05 mL of phosphate buffer and centrifuged as above. The number of cells in each fraction was determined by cell counting in a Neubauer chamber.

Glass microfiber deposition

Procyclic-stage trypanosomes at 7×10^6 cells/mL were harvested by centrifugation and re-suspended in PBS buffer. Cells were treated with 1 % (w/v) paraformaldehyde and 0.2 % (w/v) glutaraldehyde. Fixated cells were pelleted, washed with 40 vol. dH_2O and were stained (2x) with 90 mg/L Brilliant blue G250 in 7 % (v/v) HOAc for 1h at 20°C. Stained cells were washed 2x with 20 vol. dH_2O. For filter deposition, 1×10^7 cells were diluted in 5 mL dH_2O and gently pushed through a qpcore® syringe filter holder (Neolab) equipped with a Whatman GF/C glass microfibre membrane (VWR) with a particle retention cutoff of 1.2 µm (filter diameter: 25 mm). The filter membrane was covered by a custom-made Teflon washer with an 8 mm orifice. Adhered cells were rinsed with 5 mL dH_2O.

Microscopy and parasite cell counting

Parasite cells were either pre-diluted in PBS buffer or directly applied to a hematocytometer with Neubauer improved layout. Minimally three squares of the grid (each 0.1 µL) were counted for cell-density determinations. Cells were visualized with a Zeiss Primostar microscope with plan-achromat 10x and 20x objectives and imaged with an AxioCam ERc 5s (Zeiss).

Dielectric and EM sensor characterization

Measurements of cell suspensions and (un-)coated glass microfiber filters were performed in a mm-wave continuous-wave instrument consisting of a vector network analyzer and frequency extension modules for the 220 GHz to 330 GHz band. For the extraction, a model-based fitting algorithm was used, which matches the dielectric properties of a stack of N different media to fit the transmission scattering parameters to the measured data. A moving-average smoothing over up to 10 % of the captured bandwidth was applied to attenuate the effects of residual standing-wave artifacts remaining in the extracted permittivity. Measurements of sensor prototypes were recorded either in the aforementioned mm-wave setup, or in a time-domain spectrometer configured for transmission measurements at 0.15 THz to 6 THz. In the latter case, time gating was applied to reduce path reflection artifacts.

Acknowledgment: Andreas Völker is thanked for maintaining *T. b. brucei* stock cultures and Dr. Matthias Leeder for graphical input.

Funding: The authors acknowledge funding of the ApTera II project (DA1275/5-2 and GO516/7-2) by the German Research Foundation (DFG) within the national priority program SPP1857 ESSENCE.

References

[1] K. Stuart, R. Brun, S. Croft, A. Fairlamb, R. E. Gürtler, J. McKerrow, S. Reed, and R. Tarleton, "Kinetoplastids: related protozoan pathogens, different diseases," *J. Clin. Investig.*, vol. 118, no. 4, pp. 1301–1310, Apr. 2008.

[2] "WHO fact sheet no. 259 (03/2014)." [Online]. Available: http://www.who.int/mediacentre/factsheets/fs259/en/

[3] P. Büscher, G. Cecchi, V. Jamonneau, and G. Priotto, "Human African trypanosomiasis." *Lancet*, vol. 390, no. 10110, pp. 2397–2409, Nov. 2017.

[4] R. Brun, J. Blum, F. Chappuis, and C. Burri, "Human African trypanosomiasis." *Lancet*, vol. 375, no. 9709, pp. 148–159, Jan. 2010.

[5] D. Steverding, "Sleeping sickness and nagana disease caused by trypanosoma brucei," in *Arthropod borne diseases*, 1st ed., C. B. Marcondes, Ed. Cham: Springer International Publishing, 2017, pp. 277–297.

[6] R. Knieß, M. Mueh, S. Sawallich, C. B. Wagner, H. U. Göringer, C. Damm, B. Chmielak, U. Plachetka, and M. Lemme, "Towards the Development of THz-Sensors for the Detection of African Trypanosomes," *Frequenz*, vol. 72, no. 3-4, pp. 101–111, 2018.

[7] J. Mulindwa, K. Leiss, D. Ibberson, K. Kamanyi Marucha, C. Helbig, L. Melo do Nascimento, E. Silvester, K. Matthews, E. Matovu, J. Enyaru, and C. Clayton, "Transcriptomes of Trypanosoma brucei rhodesiense from sleeping sickness patients, rodents and culture: Effects of strain, growth conditions and RNA preparation methods." *PLoS Negl. Trop. Dis.*, vol. 12, no. 2, p. e0006280, Feb. 2018.

[8] S. M. Lanham, "Separation of trypanosomes from the blood of infected rats and mice by anion-exchangers." *Nature*, vol. 218, no. 5148, pp. 1273–1274, Jun. 1968.

[9] V. Lejon, P. Büscher, R. Nzoumbou-Boko, G. Bossard, V. Jamonneau, B. Bucheton, P. Truc, J.-L. Lemesre, P. Solano,

and P. Vincendeau, "The separation of trypanosomes from blood by anion exchange chromatography: From Sheila Lanham's discovery 50 years ago to a gold standard for sleeping sickness diagnosis." *PLoS Negl. Trop. Dis.*, vol. 13, no. 2, p. e0007051, Feb. 2019.

[10] W. H. Lumsden, C. D. Kimber, and M. Strange, "Trypanosoma brucei: detection of low parasitaemias in mice by a miniature anion-exchanger/centrifugation technique." *Trans. R. Soc. Trop. Med. Hyg.*, vol. 71, no. 5, pp. 421–424, 1977.

[11] J. C. M. Garnett and J. Larmor, "XII. Colours in metal glasses and in metallic films," *Philosophical Transactions of the Royal Society of London. Series A, Containing Papers of a Mathematical or Physical Character*, vol. 203, no. 359-371, pp. 385–420, 1904.

[12] M. Mueh, M. Maasch, M. Brecht, H. U. Göringer, and C. Damm, "Complex Dielectric Characterization of African Trypanosomes for Aptamer-based Terahertz Sensing Applications," in *First IEEE MTT-S International Microwave Bio Conference (IMBioC)*, May 2017, pp. 1–4.

[13] M. Mueh and C. Damm, "Spurious Material Detection on Functionalized Thin-Film Sensors using Multiresonant Split-Rings," in *IEEE International Microwave Biomedical Conference (IMBioC)*, 2018, pp. 196–198.

[14] G. S. Fiorini and D. T. Chiu, "Disposable microfluidic devices: fabrication, function, and application," *BioTechniques*, vol. 38, no. 3, pp. 429–446, 2005.

[15] M. Maasch and C. Damm, "Sensitivity improvement of split-ring resonators for thin-film sensing using floating electrodes," in *40th International Conference on Infrared, Millimeter, and Terahertz waves (IRMMW-THz)*, Aug. 2015, pp. 1–1, iSSN: 2162-2027.

[16] M. Maasch, M. Mueh, and C. Damm, "Sensor Array on Structured PET Substrates for Detection of Thin Dielectric Layers at Terahertz Frequencies," in *IEEE MTT-S International Microwave Symposium (IMS)*, Jun. 2017, pp. 1030–1033.

[17] M. Mueh, P. Hinz, and C. Damm, "Single-substrate Microfluidic Systems on PET Film for mm-Wave Sensors," in *IEEE MTT-S International Microwave Biomedical Conference (IMBioC)*, 2020, pp. 1–3.

[18] L. T. Phan, S. M. Yoon, and M.-W. Moon, "Plasma-based nanostructuring of polymers: A review," *Polymers*, vol. 9, no. 9, 2017.

[19] G. A. Cross, "Identification, purification and properties of clone-specific glycoprotein antigens constituting the surface coat of Trypanosoma brucei." *Parasitology*, vol. 71, no. 3, pp. 393–417, Dec. 1975.

[20] S. G. Grant, J. Jessee, F. R. Bloom, and D. Hanahan, "Differential plasmid rescue from transgenic mouse DNAs into Escherichia coli methylation-restriction mutants." *Proc. Natl. Acad. Sci. U.S.A.*, vol. 87, no. 12, pp. 4645–4649, Jun. 1990.

[21] B. J. Thomas and R. Rothstein, "Elevated recombination rates in transcriptionally active DNA." *Cell*, vol. 56, no. 4, pp. 619–630, Feb. 1989.

[22] R. Brun and Schönenberger, "Cultivation and in vitro cloning or procyclic culture forms of Trypanosoma brucei in a semi-defined medium. Short communication." *Acta Trop.*, vol. 36, no. 3, pp. 289–292, Sep. 1979.

[23] H. Hirumi and K. Hirumi, "Continuous cultivation of Trypanosoma brucei blood stream forms in a medium containing a low concentration of serum protein without feeder cell layers." *J. Parasitol*, vol. 75, no. 6, pp. 985–989, Dec. 1989.